

## The Effects of Water Addition on the Color and Crystalline Phase of $Y_2O_3$ Coatings Fabricated by Plasma Suspension Spray

Sang-Jun Park\*\*\*, Jung-Ki Lee\*\*\*, Yoon-Suk Oh\*, Seongwon Kim\*,  
Hyungsun Kim\*\*, and Sung-Min Lee\*†

\*Engineering Ceramic Center, Korea Institute of Ceramic Engineering and Technology, Icheon 17303, Korea

\*\*School of Material Engineering, Inha University, Incheon 22212, Korea

(Received September 23, 2016; Revised November 1, November 3, 2016; Accepted November 4, 2016)

### ABSTRACT

The effects of water addition on  $Y_2O_3$  coatings or thick films prepared by plasma suspension spray (SPS) have been investigated. Water addition in suspension media was found to be effective to control the color of a  $Y_2O_3$  coating prepared by SPS. The color changed with water addition at the shortest stand-off distance of 50 mm even if samples had the same crystalline phase. Change was not correlated with fragmentation behavior of liquid suspension inside the plasma jet. Water content over 50 vol% was found to produce unmelted particles, indicating that water suppressed heat transfer to the particles. However, plasma jet temperature was not affected. Instead, the coating fabricated with water addition has higher oxygen and lower carbon content compared to these characteristics of the coating without water addition. This was attributed to the retarded complete evaporation of liquid media from the suspension droplet, resulting in inhibition of excessive heating and evaporation of the molten  $Y_2O_3$  droplet. In this regard, crystalline phase development with respect to stand-off distance and water addition was discussed.

**Key words :** Suspension plasma spray (SPS),  $Y_2O_3$ , Water

### 1. Introduction

As transistor size has scaled down,  $Y_2O_3$  ceramics have been widely used in the semiconductor industry in order to reduce particulate contamination inside the wafer processing chamber.<sup>1-10</sup>  $Y_2O_3$  ceramics are applied as a sintered bulk or as coatings in various components because these materials have very high plasma resistance in fluorine-based plasma. To achieve  $Y_2O_3$  ceramics as coatings, various techniques such as physical vapor deposition, aerosol deposition, and plasma spray have been used.<sup>6-10</sup> Of these, suspension plasma spray (SPS) has become a new candidate method to obtain a highly dense microstructure.<sup>8,9</sup>

SPS coating generally uses submicrometer- or a few micrometer-sized powders dispersed in a liquid media as a feeding material for the plasma spray; these sizes are compared to those in materials used in the conventional plasma spray, which have a few tens of micrometer-sized granules.<sup>10,11</sup> The suspension is injected radially or axially into the plasma jet and is fragmented into small droplets; then, after evaporation of the liquid media, the particles are melted and deposited on the substrate.<sup>10,11</sup> Thus, the coatings fabricated by SPS consisted of finer splats or particles than those in coating by conventional plasma spray; also, the produced materials generally showed denser micro-

structure and smaller pores.<sup>8,9</sup>

For commercialization of coatings, color control is a key technology, though the effect of color on the production of particulate contamination is not clear. The semiconductor industry usually requires bright-colored coatings, as well as a dense microstructure. However, the processing parameters needed to obtain a dense microstructure often result in a dark gray color of the coatings: for instance, a shorter stand-off distance for coating leads to a denser microstructure, but with dark color. Colors of coatings in plasma spraying may come from many different sources such as primary particle size, dopant, crystalline phase, valance change of transition metal with reduction, vacancy formation, and deposition method.<sup>12-17</sup>

In this study, the effects of water addition to the suspension on the  $Y_2O_3$  coating have been investigated. First, we observed the color change of the coatings with respect to the stand-off distance as water is added to the suspension. Then, development of crystalline phase was observed with or without water addition. To check for the possibility of different fragmentation behavior depending on water addition, we did a single rapid scan of the plasma spray and obtained the splat size distribution. Finally, through oxygen content measurement, color and crystalline phase development were discussed.

### 2. Experimental Procedure

Fine  $Y_2O_3$  powder (> 99.95%, Grade C, H.C. Starck, Ger-

†Corresponding author : Sung-Min Lee

E-mail : smlee@kicet.re.kr

Tel : +82-31-645-1441 Fax : +82-31-645-1492

many) was dispersed in ethanol with or without water addition. The content of  $Y_2O_3$  was 2 vol% and ethanol was partially substituted with water in various levels of vol% (3, 10, 30, 50 and 100). Mixed suspension was ball-milled for 4 hr after the addition of a dispersant of 0.5 wt% (DISPER-BYK-111, BYK-Chemie GmbH, Germany).

The coating was fabricated on an alumina substrate with a diameter of 25 mm by continuous spraying using a suspension plasma spray system (Axial III, Northwest Mettech, Canada) with axial suspension feeding. The horizontal and vertical spans of the gun trajectory were 50 and 10 cm, respectively, and the vertical increment of the gun position for every horizontal movement was 5 mm. The SPS conditions were configured as follows: gas flow rate of 200 L/min with a gas composition of  $Ar/N_2/H_2$ : 45/45/10 and a plasma current of 200 A. Stand-off distance was varied between 50, 70, and 100 mm. The surface temperature of the substrate was measured using k-type thermocouples that were located on the top of alumina substrate. In order to obtain size distribution of the splats, suspension was rapidly spray-scanned once at a very fast transverse gun speed (4 m/sec) on a mirror polished soda-lime glass substrate; this process is the so-called single rapid scan. After the single rapid plasma spray test, splats were observed using a scanning electron microscope (SEM, JSM-6390, JEOL, Japan) and were analyzed with image analysis software (Image-Pro Plus, Version 6.0, Media Cybernetics Inc., USA) to obtain a splat size distribution.

The color of the coating was quantitatively measured using a UV-VIS spectrophotometer (UV-2600, Shimadzu, Japan) in the wavelength range of 380~780 nm. Crystalline phase of the coating was analyzed using an X-ray diffractometer (RINT-2500HF, Rigaku, Japan). Oxygen and carbon contents of the coating were measured using an oxygen/nitrogen analyzer (EMGA-920, Horiba, Japan) and a carbon/sulfur analyzer (CS230, LECO, USA). O/Y ratios were measured using XPS (K-Alpha, ThermoScientific, UK) with monochromatic Al K $\alpha$  radiation.

### 3. Results and Discussion

Figure 1 shows typical coated samples with respect to stand-off distance when ethanol was used as suspension media. At a stand-off distance, 50 mm, the coating surface appeared dark-gray; however, at increasing distances, the color changed to white-gray, which is the desired color in usual applications in the semiconductor industry. However, when we add water to the suspension, we were able to obtain a brighter color even at short stand-off distance. Fig. 2 shows the measured brightness, the  $L^*$  value, with respect to the stand-off distance when water of 10 vol% was added to ethanol. With the addition of water, the  $L^*$  value was around 90 even at the shortest stand-off distance, 50 mm, showing the strong effect of water on the color of the coating.

To understand this color change, we first checked the X-

ray diffraction patterns of the coatings (Fig. 3). Without water addition, at stand-off distances of 50 and 70 mm, crystalline phases mostly consisted of cubic phase while, at 100 mm, a mixture of cubic and monoclinic phases was observed (Fig. 3(a)). In contrast, when water of 10 vol% was added, the cubic phase appeared only at the stand-off distance of 50 mm. For the suspension with water of 50 vol%, similar crystalline phases were observed with respect to the stand-off distance. At ambient temperature and pressure, cubic  $Y_2O_3$  is a stable crystalline structure, while metastable monoclinic phase was usually observed after physical vapor deposition or plasma synthesis of nano powders, which can be considered as extremely fast cooling.<sup>18,19)</sup> In terms of crystalline structure, both specimens coated at the stand-off distance of 50 mm showed the same crystalline phase, regardless of the water addition, but showed different colors, implying that the color change may not be a direct result of the crystalline phase.

As another possibility, we compared the morphology and size distribution of splats, which were deposited by a single rapid scan on the glass substrate, because the water addition can affect the fragmentation behavior of the suspension liquid inside the plasma jet. Fig. 4 shows that, with an addition of water of over 50 vol%, debris from unmelted particles

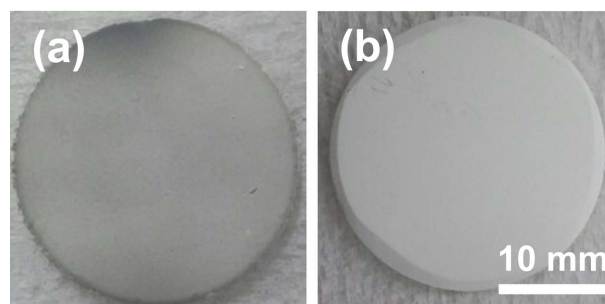


Fig. 1.  $Y_2O_3$  coatings on alumina substrate deposited at stand-off distances of (a) 50 mm and (b) 100 mm using a liquid media without water addition.

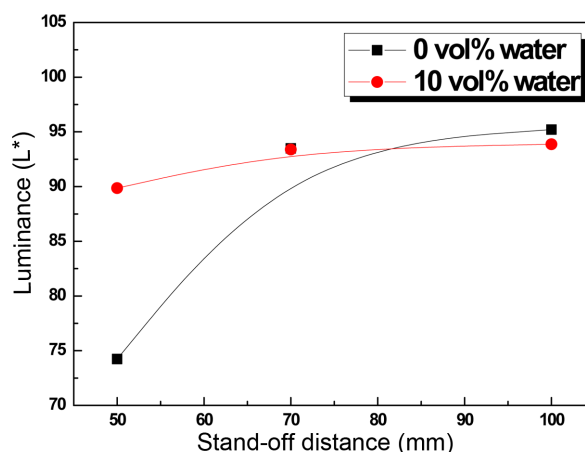


Fig. 2. Variation of brightness  $L^*$  with respect to stand-off distance for the samples fabricated without water and with water of 10 vol% in the suspension.

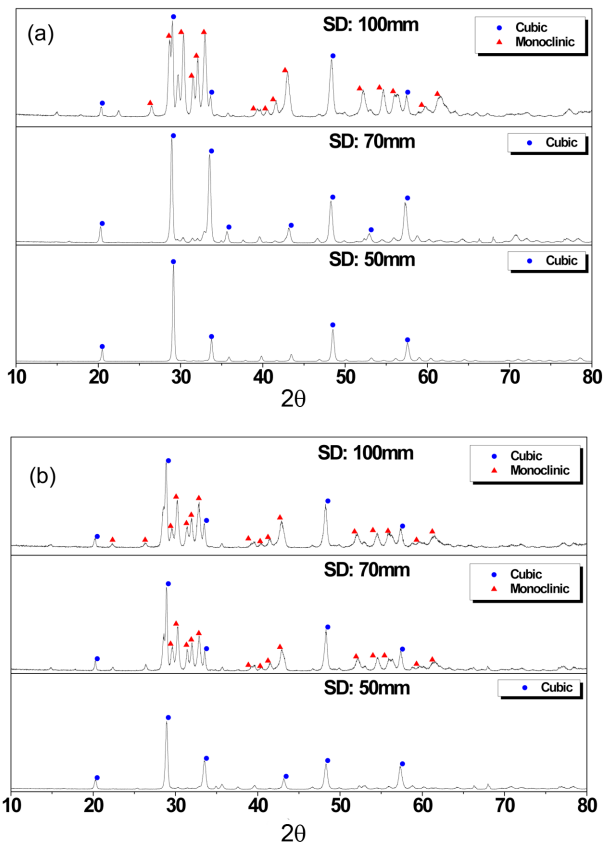


Fig. 3. XRD diffraction patterns with respect to stand-off distance: (a) without water and (b) with water of 10 vol% in the suspension.

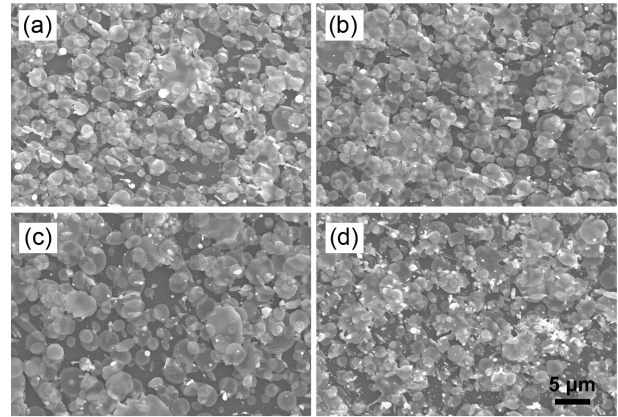


Fig. 4. SEM images after single rapid scan using suspension with water content of: (a) 3 vol%, (b) 10 vol%, (c) 30 vol%, and (d) 50 vol%.

began to appear. However, if the water was kept low enough, lower than 30 vol%, all particles melted well and showed well-developed thin disk shapes with similar sizes. Fig. 5 shows the splat size distributions obtained by image analysis with respect to water content. Regardless of the water content in the range up to 50 vol%, splat size at maximum frequency was around 1.5  $\mu\text{m}$ , indicating that water addition did not much affect the fragmentation behavior of the suspension inside the plasma jet.

On the other hand, the water addition might reduce the temperature of the plasma jet. Evaporation enthalpies of ethanol and water are 1.06 kJ/ml and 2.26 kJ/ml, respec-

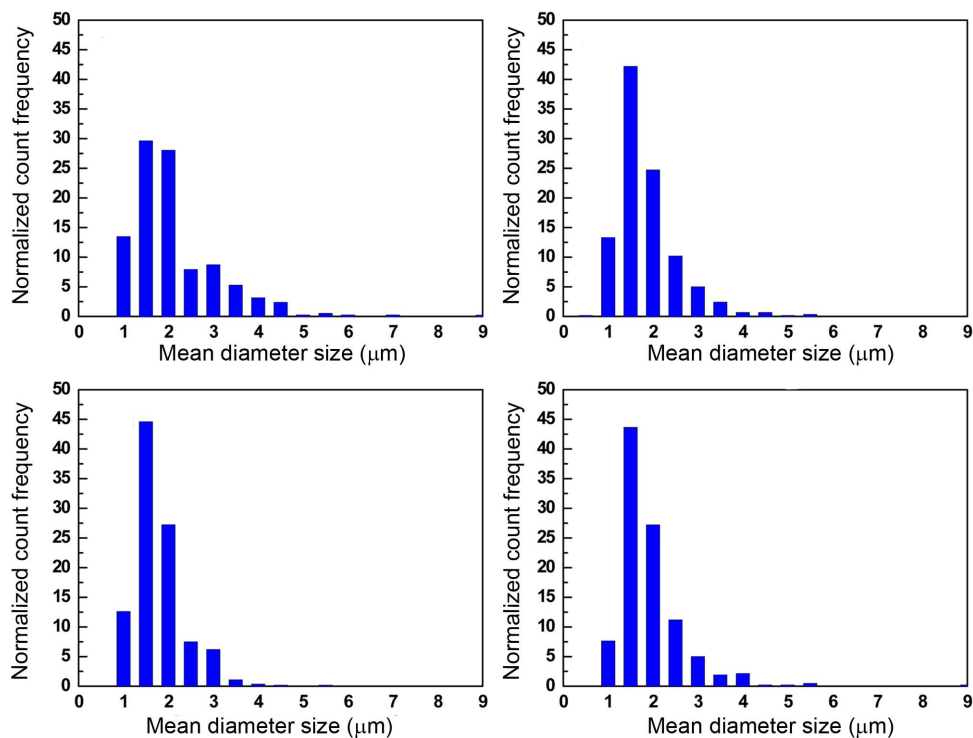


Fig. 5. Splat size distribution with water content of: (a) 3 vol%, (b) 10 vol%, (c) 30 vol%, and (d) 50 vol% in suspension.

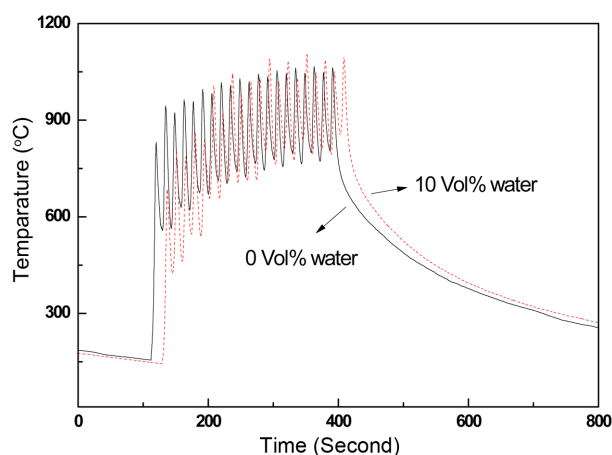


Fig. 6. Surface temperature of alumina substrate with time at stand-off distance of 50 mm.

tively.<sup>20)</sup> However, this idea of water addition reducing the temperature was rejected based on the calculation of additional enthalpy consumption due to water evaporation. The suspension flow rate in our study was fixed at 45 ml/min. With this flow rate, the additional enthalpy necessary for the evaporation of a mixture of 50 vol% water was calculated and found to be only about 0.45 kJ/sec, which was quite negligible for the typical plasma jet power used in this experiment, 80 kJ/sec. Thus, the temperature of the plasma jet must be kept nearly constant regardless of water addition. To confirm this, the heat delivered to the substrate by the plasma jet was qualitatively compared by measuring the surface temperature of the substrate with or without water addition. Fig. 6 shows the temperatures of the front surface of the substrate with coating time. Irrespective of water addition, the steady state temperature of the substrates remained the same, indicating that water addition to the suspension did not much affect the plasma jet temperature.

Instead of the plasma jet temperature, water addition can control the time for heat delivery to ceramic particles. When the sizes of the liquid droplet after fragmentation in the plasma jet were the same, as shown in Fig. 5, addition of water increases the time for the liquid in the droplet to evaporate completely. This retardation of complete liquid evaporation by water addition will reduce the length of the plasma jet zone available for melting of ceramic particles, reducing the time for heat delivery to a particle until its deposition on the substrate. By this retardation of complete liquid evaporation, water addition may be used to adjust the final temperature of molten  $Y_2O_3$  droplets. An excessive temperature of a molten ceramic droplet may induce evaporation of its components. During evaporation, cations and anions may evaporate at different speeds,<sup>21)</sup> resulting in nonstoichiometry of the coating. In order to confirm this possibility, we measured the oxygen and carbon content of coatings deposited at a stand-off distance of 50 mm (Fig. 7). The coating fabricated with water addition had higher oxy-

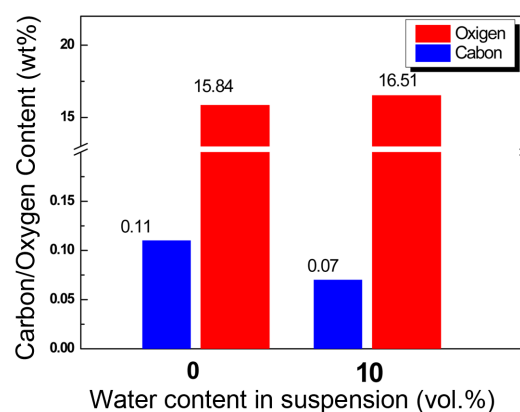


Fig. 7. Oxygen and carbon content of coatings deposited at stand-off distance of 50 mm without water and with water of 10 vol%.

gen content, supporting the idea that the water addition lowered the temperature of the molten droplet. In addition, water was also effective at removing carbon that might be introduced by polymer addition as a dispersant. It is well known that nonstoichiometry in oxides produces ionic defects,<sup>22)</sup> which can act as optical absorption sources. Carbon is also known as a traditional coloring agent. Thus, higher oxygen and lower carbon content in the coating produced with water addition seem to contribute to a brighter color of the coating.

The temperature of the molten droplet and the resultant O/Y ratio may affect the crystalline phase development. As shown in the Y-O phase diagram,<sup>23)</sup> hexagonal( $\beta$ )  $Y_2O_3$  is solidified in a temperature range between 2600 and 2718 K, while cubic( $\alpha$ )  $Y_2O_3$  is solidified below 2600 K. Because of the liquidus line in the oxygen deficient side of the  $Y_2O_3$ , a more oxygen deficient melt starts to solidify at lower temperature and may experience slow cooling, preferring a cubic crystalline phase. This might explain the crystalline phase development of the coating with respect to the stand-off distance and the water addition. As water is added, the temperature of the molten droplet is lower and the oxygen deficiency is also lower. On the other hand, with longer stand-off distance, the molten droplet undergoes faster cooling due to the lower average temperature of the substrate surface, as shown in Fig. 8. If we assume that the flight speed of a droplet in a plasma jet is 500 m/sec, the total flight time is very short, in the range of 100 msec. Then, the molten droplet might spend most of the time in concomitant evaporation before its complete solidification on the substrate. Thus, we can expect that, with water addition and longer stand-distance, the ceramic liquid melt with composition closer to stoichiometric  $Y_2O_3$  will experience faster cooling and will prefer the development of monoclinic phase development. In an opposite case, if the composition is away from stoichiometric  $Y_2O_3$  at shorter stand-off distance, the cubic crystalline phase is preferred. Indeed, as shown in the O/Y ratio of the coating without water addition (Fig. 9), the

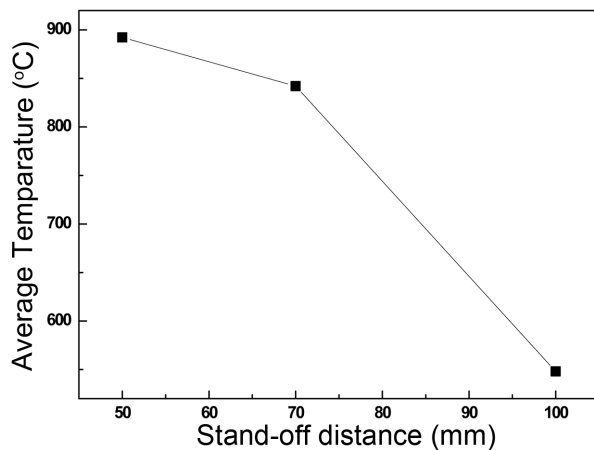


Fig. 8. Average surface temperature of alumina substrate at steady state with respect to stand-off distance for samples fabricated without water addition in suspension.

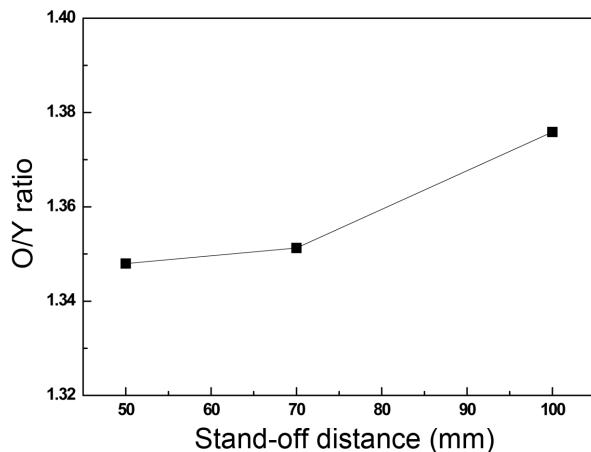


Fig. 9. O/Y ratio measured using XPS with respect to stand-off distance for samples fabricated without water addition in suspension.

ratio at the stand-off distance of 100 mm was highest; here, the monoclinic phase developed, as shown in Fig. 3, supporting our hypothesis. For this hypothesis to be more valid, we need further experimental evidence such as a direct temperature observation of a liquid droplet, optical absorption behavior, and more accurate O/Y determination. Quantitatively accurate determination of O/Y is generally very difficult because it requires accuracy for both cation and anion. This will require further study in the future.

Finally, it should be noted that, in addition to the usual processing parameters in SPS, such as plasma power, stand-off distance, and gas composition and gas flow rate, this study shows another parameter that controls the deposition process in SPS. By adjusting the water addition, we were able to control the temperature of the molten droplet independently from the other parameters. For instance, higher plasma power, which contributes to higher speed of the molten droplet and denser coating microstructure, can

be utilized along with controlling the temperature of the molten droplets by water addition. Color control could be one potential application of this study.

## 4. Conclusions

Water addition in liquid media was found to be effective at controlling the color of a  $Y_2O_3$  coating prepared by plasma suspension spray. At the shortest standoff distance, the color changed with water addition, though the coatings have the same cubic crystalline phase. Water content over 50 vol% produced unmelted particles, indicating that water suppressed heat transfer to the particles. However, the fragmentation behavior of the suspension inside the plasma jet was not affected by the water addition and the plasma jet temperature was not affected either. Instead, the coating fabricated with water addition has higher oxygen and lower carbon content compared to those characteristics of the coating without water addition. This was attributed to the retarded complete evaporation of the liquid from the suspension droplet, which reduced the length of the plasma jet zone available for heat delivery to a ceramic particle, resulting in inhibition of excessive heating and of evaporation of the molten  $Y_2O_3$  liquid droplet. In this regard, water addition seems to be an effective tool to independently control the temperature of molten liquid droplets while maintaining other parameters in a plasma spray.

## Acknowledgments

This research was supported by a grant from the Fundamental R&D Program for Core Technology of Materials funded by the Ministry of Trade, Industry and Energy, Republic of Korea.

## REFERENCES

1. M. Schaepkens, R. C. M. Bosch, T. E. F. M. Standaert, G. S. Oehrlein, and J. M. Cook, "Influence of Reactor Wall Conditions on Etch Processes in Inductively Coupled Fluorocarbon Plasmas," *J. Vac. Sci. Technol. A*, **16** 2099-107 (1998).
2. Y. Kobayashi, "Current Status and Needs in the Future of Ceramics Used for Semiconductor Production Equipment (in Japanese)"; pp. 1-7 in *Proceeding of the 37th Seminar on High-Temperature*, Ceramics Society of Japan, Osaka, 2005.
3. N. Ito, T. Moriya, F. Uesugi, M. Matsumoto, S. Liu, and Y. Kitayama, "Reduction of Particle Contamination in Plasma-Etching Equipment by Dehydration of Chamber Wall," *Jpn. J. Appl. Phys.*, **47** [5R] 3630-34 (2008).
4. G. S. May and C. J. Spanos, *Fundamentals of Semiconductor Manufacturing and Process Control*; pp. 98-102, IEEE, New Jersey 2006.
5. C. Cardinaud, M. C. Peignon, and P. Y. Tessier, "Plasma Etching: Principles Mechanisms, Application to Micro- and Nano-Technologies," *Appl. Surf. Sci.*, **164** 72-83 (2000).
6. D. M. Kim, Y. S. Oh, S. W. Kim, H. T. Kim, D. S. Lim, and

- S.-M. Lee, "The Erosion Behaviors of  $Y_2O_3$  and  $YF_3$  Coatings under Fluorocarbon Plasma," *Thin Solid Films*, **519** [20] 6698-702 (2011).
7. J. Iwasawa, R. Nishimizu, M. Tokita, and M. Kiyohara, "Plasma-Resistant Dense Yttrium Oxide Film Prepared by Aerosol Deposition Process," *J. Am. Ceram. Soc.*, **90** [8] 2327-32 (2007).
  8. J. Kitamura, Z. Tang, H. Mizuno, K. Sato, and A. Burgess, "Structural, Mechanical and Erosion Properties of Yttrium Oxide Coatings by Axial Suspension Plasma Spraying for Electronics Applications," *J. Therm. Spray Technol.*, **20** [1] 170-85 (2011).
  9. S. J. Kim, J. K. Lee, Y. S. Oh, S. W. Kim, and S. M. Lee, "Effect of Processing Parameters and Powder Size on Microstructures and Mechanical Properties of  $Y_2O_3$  Coatings Fabricated by Suspension Plasma Spray," *J. Korean Ceram. Soc.*, **52** [6] 395-402 (2015).
  10. P. Fauchais and G. Montavon, "Latest Developments in Suspension and Liquid Precursor Thermal Spraying," *J. Therm. Spray Technol.*, **19** [1-2] 226239 (2010).
  11. C. Delbos, J. Fazilleau, V. Rat, J. F. Coudert, P. Fauchais, and B. Pateyron, "Phenomena Involved in Suspension Plasma Spraying Part 2: Zirconia Particle Treatment and Coating Formation," *Plasma Chem. Plasma Process*, **26** 393-414 (2006).
  12. J. Kitamura, H. Mizuno, N. Kato, and I. Aoki, "Plasma-Erosion Properties of Ceramic Coating Prepared by Plasma Spraying," *J. Jpn Thermal Spray Soc.*, **47** [7] 1677-83 (2006).
  13. J. R. Nicholls, K. J. Lawson, A. Johnstone, and D. S. Rickerby, "Methods to Reduce the Thermal Conductivity of EB-PVD TBCs," *Surf. Coat. Technol.*, **151-152** 383-91 (2002).
  14. S. Dosta, M. Torrell, I. G. Cano, and J. M. Guilemany, "Functional Colored Ceramic Coatings Obtained by Thermal Spray for Decorative Application," *J. Eur. Ceram. Soc.*, **32** [14] 3685-92 (2012).
  15. P. Ctibor, Z. Pala, J. Sedláč, V. Štengl, I. Píš, T. Zahanová, and V. Nehasil, "Titanium Dioxide Coating Sprayed by a Water Stabilized Plasma Gun (WSP) with Argon and Nitrogen as the Powder Feeding Gas : Differences in Structural Mechanical and Photocatalytic Behavior," *J. Therm. Spray Tech.*, **21** [3] 425-34 (2012).
  16. G. M. Ingo, "Origin of Darkening in 8 wt% Yttria-Zirconia Plasma-Sprayed Thermal Barrier Coatings," *J. Am. Ceram. Soc.*, **74** [2] 381-86 (1991).
  17. M. J. Kelly, D. E. Wolfe, J. Singh, and J. Eldridge, "Thermal Barrier Coating Design with Increased Reflectivity and Lower Thermal Conductivity for High-Temperature Turbine Applications," *Int. J. Appl. Ceram. Technol.*, **3** [2] 81-93 (2006).
  18. M. Hartmanova, M. Jergel, J. P. Holgado, and J. P. Espinos, "Structure and Microstructure of EB-PVD Yttria Thin Films Grown on Si (111) Substrate," *Vacuum*, **85** 535-40 (2010).
  19. X. L. Sun, A. I. Y. Tok, S. L. Lim, F. Y. C. Boey, C. W. Kang, and H. W. Ng, "Combustion-aided Suspension Plasma Spraying of  $Y_2O_3$  Nanoparticles: Synthesis and Modeling," *J. App. Phys.*, **103** [3] 04308 (2008).
  20. W. M. Haynes, CRC Handbook of Chemistry and Physics; CRC Press, USA, 2016.
  21. M. Ohring, Materials Science of Thin Films; Academic Press, USA, 2002.
  22. J. Maier, Physical Chemistry of Ionic Materials; John Wiley & Sons, UK, 2004.
  23. D. Djurovic, M. Zinkevich, and F. Aldinger, "Thermodynamic Modeling of the Yttrium-Oxygen System," *Calphad*, **31** 560-66 (2007).